

1 **Mycorrhizal distributions impact global patterns of carbon and nutrient cycling**

2 **R. K. Braghiere^{1,2†}, J. B. Fisher^{1,2}, R. A. Fisher^{3,4}, M. Shi^{1,2}, B. S. Steidinger⁵, B. N.**
3 **Sulman⁶, N. A. Soudzilovskaia⁷, X. Yang⁶, J. Liang^{8,9}, K. G. Peay⁵, T. W. Crowther¹⁰, R. P.**
4 **Phillips¹¹**

5 ¹ Jet Propulsion Laboratory, California Institute of Technology, 4800 Oak Grove Drive,
6 Pasadena, CA, 91109 USA.

7 ² Joint Institute for Regional Earth System Science and Engineering, University of California at
8 Los Angeles, Los Angeles, CA, 90095 USA.

9 ³ Climate and Global Dynamics Division, National Center for Atmospheric Research, Boulder,
10 CO, USA.

11 ⁴ Laboratoire Évolution & Diversité Biologique, CNRS:UMR 5174, Université Paul Sabatier,
12 Toulouse, France.

13 ⁵ Department of Biology, Stanford University, Stanford, CA, USA.

14 ⁶ Environmental Sciences Division and Climate Change Science Institute, Oak Ridge National
15 Laboratory, Oak Ridge, TN, USA.

16 ⁷ Environmental Biology Department, Institute of Environmental Sciences, Leiden University,
17 Leiden, The Netherlands.

18 ⁸ Department of Forestry and Natural Resources, Purdue University, West Lafayette, IN, USA.

19 ⁹ Research Center of Forest Management Engineering of State Forestry and Grassland
20 Administration, Beijing Forestry University, Beijing, China.

21 ¹⁰ Department of Environmental Systems Science, ETH Zürich, Zürich, Switzerland.

22 ¹¹ Department of Biology, Indiana University, 1001 E Third St, Bloomington, IN 47403, USA.

23

24 Corresponding author: Dr. Renato K. Braghiere (renato.k.braghiere@jpl.nasa.gov)

25 † Current address: Jet Propulsion Laboratory, M/S 233-305F, 4800 Oak Grove Drive, Pasadena,
26 CA, 91109 USA.

27 **Key Points:**

- 28 • Global plant demand for N has increased 25% from 1850 to 2010, while the C cost
29 associated with it has increased 60% in the same period.
- 30 • NPP has increased by 20% from 1850 to 2010, but the NPP fraction used for nitrogen
31 acquisition increased from $\sim 1/4$ to $\sim 1/3$.
- 32 • Areas of savannas and forest-grasslands transition zones present a higher risk of nitrogen
33 limitation to plant growth.

34

35 **Keywords:**

- 36 • Biogeochemistry, carbon cycling, climate change, Earth System modeling, mycorrhizae,
37 nutrient cycling

38 **Abstract**

39 Most tree species predominantly associate with a single type of mycorrhizal fungi, which can
40 differentially affect plant nutrient acquisition and biogeochemical cycling. Here, we address for
41 the first time the impact of mycorrhizal distributions on global carbon and nutrient cycling.
42 Using the state-of-the-art carbon-nitrogen economics within the Community Land Model version
43 5 (CLM5) we found Net Primary Productivity (NPP) increased throughout the 21st century by
44 20%; however, as soil nitrogen has progressively become limiting, the costs to NPP for nitrogen
45 acquisition — i.e., to mycorrhizae — have increased at a faster rate by 60%. This suggests that
46 nutrient acquisition will increasingly demand a higher portion of assimilated carbon to support
47 the same productivity. Uncertainties in mycorrhizal distributions are non-trivial, however, with
48 uncertainties in NPP by up to 345 Tg C yr⁻¹, depending on which published distribution is used.
49 Remote sensing capabilities for mycorrhizal detection show promise for refining these estimates
50 further.

51

52 **Plain Language Summary**

53 The majority of plants often join forces with specific types of fungi to improve their nutrient
54 acquisition capacity, which ultimately impact global photosynthesis. This is the first study to
55 explore the impacts of different types of fungi-root distributions on global carbon and nutrient
56 cycling. Using the land component of a state-of-the-art Earth System model we found that global
57 net carbon uptake increased throughout the 21st century by 20%, while the carbon spent on
58 nitrogen acquisition has increased at a faster rate by 60%. This study suggests that nutrient
59 acquisition by plants will increasingly demand a larger portion of net carbon to support the same
60 photosynthesis.

61

62

63

64 **1 Introduction**

65 Terrestrial ecosystems have been a persistent post-industrial carbon sink, absorbing
66 almost a third of anthropogenic carbon emissions (Ciais et al., 2013; Schimel et al., 2015;
67 Friedlingstein et al., 2019). Studies suggest that terrestrial ecosystem productivity has increased
68 due to elevated CO₂ concentration (Keenan et al., 2016; Zhu et al., 2016; Chen et al., 2019), but
69 it remains unclear whether this will translate to increases in the terrestrial carbon sink in the
70 future (Friedlingstein et al., 2006, 2014; Zhang et al., 2019). It is widely expected that limiting
71 factors such as water (Trenberth et al., 2014; Kolus et al., 2019) and nutrients availability
72 (Zaehle et al., 2010; Fleischer et al., 2019; Terrer et al., 2019; Wieder et al., 2015, 2019) might
73 mediate the responses of terrestrial ecosystems to climate change. Disentangling these
74 mechanisms and exploring the consequences of atmospheric CO₂ increase requires assessment of
75 such mechanisms through Earth System models (ESMs), which allow comprehensive and
76 spatially explicit assessment of the impacts of future climate on biogeochemical cycles in
77 terrestrial ecosystems.

78 It has been estimated that a large part of plant nitrogen and phosphorus is provided by
79 fungal root symbionts (van der Heijden et al., 2015), thus it is likely that mycorrhizal
80 associations explain a large fraction of the variance in plant response to elevated CO₂ (Drake et
81 al., 2011; Orwin et al., 2011; Kivlin et al., 2013; Sulman et al., 2017; Terrer et al., 2016, 2018).
82 However, the global spatial distributions of these mechanisms as well as their potential impacts
83 are still uncertain (Norby et al., 2017; Sulman et al., 2019). Only a handful of ESMs consider
84 mycorrhizal nutrient acquisition when calculating carbon assimilation and allocation (Wang et
85 al., 2010; Zaehle et al., 2015; Goll et al., 2017). The Community Land Model version 5 (CLM5)
86 within the Community Earth System Model (CESM) currently enables an explicit representation
87 of the functional differences between different types of plant symbiotic associations (Fisher et
88 al., 2010; Brzostek et al., 2014; Shi et al., 2016; Fisher et al., 2019; Lawrence et al., 2019).
89 However, until recently, one of the major challenges in generating global estimates of nutrient
90 limitation on the global carbon cycle is related to a lack of understanding of the spatial
91 distribution of nutrient-acquiring plant-microbe symbioses. Despite the availability of regional
92 maps of present and past plant symbiotic status (Menzel et al., 2016; Swaty et al., 2016;
93 Brundrett, 2017; Jo et al., 2019), scientists have only recently begun to develop explicit global
94 data about mycorrhizal and nitrogen fixing associations (Davies-Barnard et al., 2020).

95 Recently, scientists developed methods for extrapolating spatially sparse measurements
96 into large-scale, spatially explicit maps suitable for applications within ESMs (Shi et al., 2016;
97 Soudzilovskaia et al., 2019; Steidinger et al., 2019; Sulman et al., 2019). These developments for
98 the first time enable examining how mycorrhizal distributions are related to the global carbon
99 and nitrogen cycles. In this study, we seek a better understanding of mycorrhizas on global
100 carbon and nitrogen cycles through incorporating multiple state-of-the-art spatial distributions of
101 mycorrhizal associations in a global ecosystem model. We first compare four existing global data
102 products of global spatial distributions of mycorrhizal associations. Second, we perform transient
103 global runs of CLM5 with increasing CO₂ concentration through the 20th and 21st centuries in
104 order to understand the impact of the CO₂ fertilization effect combined with different spatially
105 variable mycorrhizal representations. Finally, we evaluate the possible feedback effects that
106 changes in spatial mycorrhizal association due to climate change (Steidinger et al., 2019) may
107 have on the global carbon cycle.

108 **2 Materials and Methods**

109 2.1 Land Surface Model description: CLM5

110 CLM5 includes the Fixation and Uptake of Nitrogen (FUN) module calculating the
111 carbon costs for each pathway of plant nitrogen uptake - symbiotic nitrogen fixation, direct and
112 mycorrhizal uptake of soil nitrogen, and nitrogen retranslocation from leaves (Fisher et al., 2010;
113 Brzostek et al., 2014; Shi et al., 2016; Allen et al., 2020). Plants shift uptake pathways to
114 minimize the carbon costs of nitrogen uptake. FUN simulates uptake from the two major types of
115 fungi that plants associate with: arbuscular mycorrhizal (AM) and ectomycorrhizal (ECM) fungi.
116 Explicit representation of mycorrhizal associations improved the dynamic predictions of the
117 nitrogen retranslocated from leaves and taken up from the soil in previous ecosystem-scale
118 studies (Brzostek et al., 2014).

119 In order to generate the trade-offs between AM, ECM, and non-mycorrhizal root uptake,
120 FUN within CLM5 uses an estimate of the percentage of aboveground biomass per grid cell that
121 associates with each mycorrhizal type (Brzostek et al., 2014; Shi et al., 2016).

122 2.2 Coupling mycorrhizae spatial distribution into CLM5

123 Plant Functional Types (PFTs) are used to classify plants according to their physical,
124 phylogenetic, and phenological characteristics. The value of each parameter is determined or
125 inferred from observable characteristics. A spatial data product can be added as a 2D variable
126 varying as function of latitude and longitude, but because land surface models also work with the
127 concept of PFTs, adding a third dimension (i.e., latitude, longitude, and PFT) into the spatial
128 distribution can improve accuracy of processes and reduce model uncertainty (Braghiere et al.,
129 2019). Here, given new datasets of spatial distributions of mycorrhizal associations based on
130 observations at different spatial resolutions, we modified CLM5 and added mycorrhizal
131 association types per PFT within a gridcell (latitude and longitude) to also consider landscape
132 heterogeneity within a model grid cell.

133 Four global maps of mycorrhizal association based on different assumptions and spatial
134 resolutions were used to provide the percentage of ECM association (relative to AM) data for
135 CLM5: Map A (Shi et al., 2016); Map B (Sulman et al., 2019), Map C (Steidinger et al., 2019),
136 and Map D (Soudzilovskaia et al., 2019) (see **Fig. 1** and **Supplementary information** for
137 details).

138 2.3 Simulation protocols

139 First, for each ECM map, initial ecosystem carbon and nitrogen stocks for 1850 were
140 generated using a spin-up approach using 1850 concentrations of CO₂ (284.7 ppm) and the
141 model's standard climate forcing dataset from the Global Soil Wetness Project Phase 3 version 1
142 (GSWP3v1) (Kim, 2017) at 1.9°x2.5° spatial resolution. The Model for Scale Adaptive River
143 Transport (MOSART) was turned on and ice evolution on land was turned off. Model runs were
144 performed with biogeochemistry mode on without crops for 200 years in 'accelerated
145 decomposition' mode (see Lawrence et al. (2019) for details) by cycling through the 1901–1920
146 climate forcing dataset and then for 400 years in regular spin-up mode until soil and plant carbon
147 and nitrogen stocks achieved steady state. Historical simulation was performed from 1850 to
148 2010 using transient GSWP3 climate, nitrogen deposition, and variable atmospheric CO₂
149 concentration.

150 Second, in order to illustrate the model sensitivity to changes in global spatial patterns of
 151 plant symbiosis due to climate change, we used a projected map of plant symbiotic status for
 152 2070 using a relative concentration pathway (RCP) of 8.5 W.m⁻² from Steidinger et al. (2019)
 153 versus the original map with present climate (Steidinger et al., 2019). We performed future runs
 154 (2015-2070) with the biogeochemistry mode on following the Shared Socio-Economic Pathway
 155 (SSP) number 5 (Kriegler et al., 2017). SSP5 scenarios are the only ones resulting in a radiative
 156 forcing pathway as high as the highest RCP8.5 used by Steidinger et al. (2019).

157 The SSP5 scenario includes extreme levels of fossil fuel use, up to a doubling of global
 158 food demand, and up to a tripling of energy demand and greenhouse gas emissions over the
 159 course of the century, marking the upper end of the scenario literature in several dimensions. We
 160 used future climatological forcing from the CESM2 simulation for the CMIP6 (Lawrence et al.,
 161 2016; O'Neill et al., 2016). We used the LMWG diagnostics package from NCAR
 162 (http://github.com/NCAR/CESM_postprocessing) and Python scripts to evaluate the differences
 163 between each model run with CLM5.

164 2.4 Calculating nitrogen limitation

165 The risk of nitrogen limitation (NL) can be determined by evaluating if the growth rate
 166 of NPP used for nitrogen uptake with time is larger than the growth rate of total NPP with time.
 167 If the amount of NPP used for nitrogen uptake increases at a higher rate than the total NPP for a
 168 particular grid cell, that grid cell is considered to be at risk of spending too much carbon on
 169 nitrogen acquisition, and therefore, NL is closer to 1. On the contrary, if the amount of NPP used
 170 for nitrogen uptake increases at a lower rate than the total NPP for a particular grid cell, that area
 171 is not considered to be at risk of spending too much carbon on nitrogen acquisition. NL is
 172 calculate as:

$$173 \quad NL = 1. - \frac{\alpha_1(i,j)}{\alpha_2(i,j)} \quad (1.0)$$

174 where α_1 is the slope of the linear regression of NPP used for Nitrogen uptake per gridcell
 175 (NPP_NUPTAKE(i,j)) with time and α_2 is the slope of the linear regression of NPP (NPP(i,j))
 176 plus NPP_NUPTAKE(i,j) with time. Areas in red indicate higher risk of nitrogen limitation on
 177 NPP based on the period from 1850 to 2010.

178 3 Results and Discussion

179 3.1 Different estimates of plant symbiotic status and impacts on nitrogen uptake 180 pathways

181 To better visualize the differences from maps presented in **Fig.1**, the standard deviation
182 of the averaged difference between ECM fraction (%) of each one of the new maps and the
183 default CLM5 map is shown in **Fig. 1e**. All three data products agree that the default map in
184 CLM5 overestimates ECM fraction in the boreal regions, as well as drier areas of the world, such
185 as the Atacama, Namibian, Somalian, Mongolian, Sonoran, and Australian deserts. Map C
186 resembles the default CLM5 map A, indicating an alignment of the assumptions that climate
187 variables are the main drivers of global biogeography of forest-tree symbioses and the
188 proposition that fixed values of mycorrhizal associations can be prescribed following PFTs
189 spatial distributions. The three maps disagree in the eastern USA, where map B indicates map A
190 overestimates ECM fraction, map C indicates the opposite, and map D shows small differences.
191 Over eastern Asia, the maps also disagree in the sign of changes of ECM fraction with respect to
192 map A. Map B shows no particular differences in Northeast China, map C indicates that map A
193 underestimates ECM fraction, while map D indicates the opposite. In central Europe, map C
194 strongly (+40%) revises the default CLM5 ECM fraction upwards, while maps B and D show a
195 much smaller positive difference in comparison to map A, except for parts of the Alps and parts
196 of the Iberic peninsula. Given that the map A is based on PFT values, the biases in particular
197 PFTs are presented in **Supplementary Fig. S1**.

198 Although all four maps agree in approximately 60% of the world area, some areas present
199 large standard deviation values ($> 30\%$), e.g., northern North America, throughout northern and
200 eastern Asia, as well as parts of the tropical forests, i.e., northwest Amazon, the central part of
201 the Congo Basin, and parts of the maritime continent. These areas would benefit from more field
202 measurements of mycorrhizal association and further analysis.

203 Throughout all runs, the ECM-associated (NECM) and AM-associated (NAM) vegetation
204 nitrogen uptake fluxes were the most impacted biogeochemical variables when including
205 spatially explicit mycorrhizal status in CLM5, though the other nitrogen uptake pathways and
206 their associated carbon costs were also impacted. There are four different representations of
207 nitrogen acquisition pathways within CLM5: mycorrhizal uptake (NMYC), nitrogen fixation

208 (NFIX), nitrogen retranslocation from leaves (NRETRANS), and the non-mycorrhizal or direct
209 nitrogen uptake (NNONMYC). The sum of all different nitrogen acquisition pathways is the total
210 acquired nitrogen (TOTALN). **Table S2** shows the average carbon cost per unit of nitrogen
211 (gN.kgC^{-1}) in the period 2000-2010 for each different nitrogen uptake pathway as predicted by
212 CLM5.

213 On average for the period 2000-2010, the updated carbon cost per unit of nitrogen
214 according to the three observation based maps (B,C, and D) increases 2.2%. The main areas
215 where carbon costs of nitrogen uptake became higher are: (i) eastern North America, Europe,
216 southeast Asia, and the tropics for mycorrhizal uptake; tropical and boreal forests for nitrogen
217 fixation; and the tropics for nitrogen retranslocation (see **Supplementary material**). Changes in
218 carbon costs of nitrogen acquisition via mycorrhizae uptake are 4.1% higher globally.

219 3.2 The effect of climate change and CO_2 fertilization on nitrogen limitation

220 To determine the climate change effect of nitrogen limitation on plant growth, **Fig. 2**
221 shows the global total NPP (PgC.yr^{-1}), global total carbon cost of nitrogen uptake
222 (NPP_NUPTAKE , PgC.yr^{-1}), global plant nitrogen demand (PLANT_NDEMAND , TgN.yr^{-1}),
223 and the global total nitrogen uptake (NUPTAKE , TgN.yr^{-1}). Nitrogen demand is calculated as the
224 total nitrogen that would be required if all assimilated carbon was allocated according to
225 idealized stoichiometric ratios. The CO_2 fertilization effect, with nitrogen deposition, and climate
226 change increased photosynthetic rates across the globe, represented by an increase in NPP from
227 40 PgCyr^{-1} in 1850 to 47.5 PgCyr^{-1} in 2010, an increase of about 20%. In turn, to support
228 elevated productivity, plants require more nitrogen, leading to an increase in plant nitrogen
229 demand from $\sim 1600 \text{ TgN.yr}^{-1}$ in 1850 to 2000 TgN.yr^{-1} in 2010, an increase of about 25%.

230 Although the rates of nitrogen uptake systematically increase in response to a higher
231 nitrogen demand, i.e., NUPTAKE of 800 TgN.yr^{-1} in 1850 to 1000 TgN.yr^{-1} in 2010, the
232 associated carbon cost of nitrogen acquisition increased at a faster rate, growing roughly 60%
233 more expensive in 2010 (17.5 PgCyr^{-1}) than it was in 1850 (11.2 PgCyr^{-1}). In terms of the
234 percentage of NPP spent in nitrogen acquisition, the values increased from about $\sim 27.5\%$ of NPP
235 in 1850 to $\sim 32.5\%$ of NPP in 2010. By 2075, it is projected that the NPP used for nitrogen
236 acquisition will reach 35% of total NPP ($\sim 22.5 \text{ PgCyr}^{-1}$), suggesting ecosystems will have much
237 less carbon available for allocation and plant growth, possibly becoming more susceptible to

238 extreme events that require extra carbon for re-growth, such as droughts, fires, and insect
 239 outbreaks.

240 All transient runs from 1850 to 2010 with the new maps indicated a stronger effect of
 241 climate and CO₂ fertilization on nitrogen limitation compared to map A. These findings highlight
 242 that as estimated by CLM5, not only has plant demand for nitrogen increased at a faster rate than
 243 actual nitrogen uptake, but that the carbon costs associated with nitrogen acquisition have
 244 increased at a faster rate than the extra carbon gained through the CO₂ fertilization effect, i.e.,
 245 plants need to invest more carbon per unit of nitrogen uptaken. This pattern is projected to
 246 continue in the future, which means that it is unlikely current plant growth rates will be sustained
 247 globally.

248 **Fig. 3a** shows the risk of nitrogen limitation (NL) calculated as described in **Eq. 1**.
 249 According to the transient runs from 1850 to 2010 using the default CLM5 map A, tropical
 250 forests have a medium to low risk of being further limited by nitrogen, which is in agreement to
 251 some studies indicating that intact ancient tropical forests tend to accumulate and recycle large
 252 quantities of nitrogen relative to temperate forests (Hedin et al., 2009).

253 A part of South America, Africa, and Australia, associated with savannas and forest-
 254 grassland transition zones present a higher risk of nitrogen limitation to plant growth. Parts of the
 255 temperate forests in North America, Europe, and Asia, as well as northern areas of the planet in
 256 the presence of boreal forests present a medium to high risk of nitrogen limitation.

257 3.3 The feedback impacts of mycorrhizal changes due to climate change

258 Recent evidence suggests that anthropogenic influences, primarily nitrogen deposition
 259 and fire suppression, as well as climate change have increased AM tree dominance during the
 260 past three decades in the eastern United States (Jo et al., 2019). Globally, Steidinger et al. (2019)
 261 presented a study using the same environment-mycorrhizae relationships for current climate to
 262 project potential changes in the symbiotic status of forests in the future, suggesting that projected
 263 climate for 2070 reduces the abundance of ECM trees by as much as 10%, with major changes in
 264 ECM abundance along the boreal–temperate transition zone (**Fig. 3b**).

265 Although the magnitude of the time lag between climate change and ecosystem responses
 266 is unknown, the predicted decline in ECM trees aligns with previous simulated warming

267 experiments, which have demonstrated that some important ECM hosts decline at the boreal–
268 temperate zones under future climate conditions (Reich et al., 2015), and that ECM fungi
269 demonstrated increased responses of mycorrhizal fungal biomass under eCO₂ compared to AM
270 fungi (Dong et al., 2018), as the simulated response in the tropics (**Fig. 3b**).

271 Although it has been previously reported that climate change should impact forest
272 symbiosis, no study has ever evaluated the potential feedback of climate change effects on
273 mycorrhizal distribution onto nitrogen and carbon cycles. The difference in NPP for the period of
274 2016-2075 between the simulations using the future maps of ECM fraction and the simulations
275 using the present-day map C (Steidinger et al., 2019) are shown in **Fig. 3c**.

276 Large parts of South America, especially areas associated with savannas, present the
277 largest negative feedback effects on NPP due to future climate change impacts on mycorrhizal
278 association, followed by areas with boreal forests. The impact over tropical forests and areas in
279 China seem to benefit from a change in plant symbiotic status in the future. Although, these
280 results should be interpreted carefully due to the limitation of the original forest plot training data
281 in those areas of the globe used in Steidinger et al. (2019), machine learning algorithms indicate
282 more ECM fungi in the tropics in the future, possibly due to the effect eCO₂ on the tropical
283 climate.

284 In the SSP5-RCP8.5 runs from 2016 to 2075 with present-day plant symbiotic status, the
285 growth rate of nitrogen uptake was 4.8 TgN.yr⁻². In terms of carbon costs, NPP is projected to
286 increase at a rate of 265.5 TgC.yr⁻², while the carbon cost of nitrogen acquisition is projected to
287 increase at a rate of 130.4 TgC.yr⁻², an extra 135.2 TgC.yr⁻¹. The feedback effect of climate
288 change on the spatial distribution of plant symbiotic status decreases NPP globally (from 58.3
289 PgC.yr⁻¹ to 58.2 PgC.yr⁻¹), a negative impact of -23.1 TgC.yr⁻¹. The projected NPP increase rate
290 with the future plant symbiotic status map is 266.2 TgC.yr⁻², 0.7 TgC.yr⁻² faster than the
291 projected NPP without changes in mycorrhizae associations. However, the carbon cost of
292 nitrogen acquisition is projected to increase at a rate of 129.1 TgC.yr⁻², versus 130.0 TgC.yr⁻² in
293 the simulations without changes in the spatial distribution of plant symbiotic status. In terms of
294 total NPP globally, these changes are predicted to increase carbon costs of nitrogen acquisition
295 by 582.5 TgC.yr⁻¹, which significantly amplifies the effect of nutrient limitation on plant growth
296 worldwide.

297 **4 Conclusions**

298 To overcome the lack of global spatial representations of mycorrhizal associations, a few
299 studies (Soudzilovskaia et al., 2019; Steidinger et al., 2019; Sulman et al., 2019) have combined
300 a comprehensive quantitative evaluation of mycorrhizae distribution across biomes and
301 continents, and assembled high-resolution digital maps of the global distribution of biomass
302 fractions of different types of mycorrhizae associations.

303 In our analysis, we show that differences between data products have impacts upon the
304 nitrogen and carbon cycles in CLM5. Nonetheless, this comparison did not aim to determine
305 which map is the most realistic. Rather, we assessed the impact of different mycorrhizal
306 representations in CLM5 to determine signs of changes in the global nitrogen and carbon cycles.
307 In this study, we found a negative impact on future NPP due to feedback effects of climate
308 change and CO₂ fertilization on mycorrhizae spatial distribution.

309 Although the transient runs with different spatial representations of plant symbiotic status
310 do not agree in terms of total values of nitrogen acquisition through different uptake pathways, or
311 their relative carbon costs, all experiments using the observation based maps do agree that the
312 increasing rate of plant nitrogen demand is higher than the rate of nitrogen uptake as previously
313 reported. Moreover, our simulations found that the carbon costs of nitrogen acquisition also
314 increase at a higher rate than NPP itself, indicating that plants need to invest more carbon per
315 unit of nitrogen uptake to sustain growth at current rates globally. To our knowledge, this is the
316 first study using observation-derived global maps of mycorrhizal association within an ESM to
317 estimate the impacts of climate change on mycorrhizas and its feedback on the global carbon and
318 nitrogen cycles.

319 **Author Contributions**

320 **Conceptualization:** R. K. Braghiere, J. B. Fisher, R. P. Phillips. **Formal analysis:** R. K.
321 Braghiere, J. B. Fisher, R. A. Fisher. **Funding acquisition:** J. B. Fisher, X. Yang, J. Liang, K. G.
322 Peay, T. W. Crowther, R. P. Phillips. **Investigation:** R. K. Braghiere, J. B. Fisher.
323 **Methodology:** R. K. Braghiere, J. B. Fisher, R. A. Fisher, M. Shi, B. N. Sulman, N. A.
324 Soudzilovskaia, X. Yang, R. P. Phillips. **Supervision:** J. B. Fisher, X. Yang. **Validation:** M. Shi,
325 B. S. Steidinger, B. N. Sulman, N. A. Soudzilovskaia, J. Liang, K. G. Peay, T. W. Crowther.

326 **Writing – original draft:** R. K. Braghiere, J. B. Fisher. **Writing – review & editing:** R. K.
327 Braghiere, J. B. Fisher, R. A. Fisher, M. Shi, B. S. Steidinger, B. N. Sulman, N. A.
328 Soudzilovskaia, X. Yang, J. Liang, K. G. Peay, T. W. Crowther, R. P. Phillips.

329 **Acknowledgments**

330 This research was carried out at the Jet Propulsion Laboratory, California Institute of
331 Technology, under a contract with the National Aeronautics and Space Administration.
332 California Institute of Technology. Government sponsorship acknowledged. This material is
333 based upon work supported by the U.S. Department of Energy, Office of Science, Office of
334 Biological and Environmental Research, Terrestrial Ecosystem Science program under Award
335 Numbers DE-SC0008317 and DE-SC0016188. Funding was also provided by the NASA IDS
336 program. Copyright 2021. All rights reserved. We would like to acknowledge high-performance
337 computing support from Cheyenne (NCAR, 2020) provided by NCAR's Computational and
338 Information Systems Laboratory, sponsored by the National Science Foundation.

339 **Data and code availability**

340 A patch file with the modified version of CLM5 and all python scripts used for analyses and
341 plots are available in <https://doi.org/10.6084/m9.figshare.12919385.v1>.

342 **References**

- 343 Allen, K., Fisher, J. B., Phillips, R. P., Powers, J. S., & Brzostek, E. R. (2020). Modeling the
344 Carbon Cost of Plant Nitrogen and Phosphorus Uptake Across Temperate and Tropical
345 Forests. *Frontiers in Forests and Global Change*, 3.
346 <https://doi.org/10.3389/ffgc.2020.00043>
- 347 Braghiere, R. K., Quaife, T., Black, E., He, L., & Chen, J. M. (2019). Underestimation of Global
348 Photosynthesis in Earth System Models Due to Representation of Vegetation Structure.
349 *Global Biogeochemical Cycles*, 33(11), 1358–1369. <https://doi.org/10.1029/2018GB006135>
- 350 Brundrett, M. C. (2017). Distribution and Evolution of Mycorrhizal Types and Other Specialised
351 Roots in Australia (pp. 361–394). https://doi.org/10.1007/978-3-319-56363-3_17
- 352 Brzostek, E. R., Fisher, J. B., & Phillips, R. P. (2014). Modeling the carbon cost of plant nitrogen

353 acquisition: Mycorrhizal trade-offs and multipath resistance uptake improve predictions of
354 retranslocation. *Journal of Geophysical Research: Biogeosciences*, 119(8), 1684–1697.
355 <https://doi.org/10.1002/2014JG002660>

356 Chen, C., Park, T., Wang, X., Piao, S., Xu, B., Chaturvedi, R. K., et al. (2019). China and India
357 lead in greening of the world through land-use management. *Nature Sustainability*, 2(2),
358 122–129. <https://doi.org/10.1038/s41893-019-0220-7>

359 Ciais, P., Sabine, C., Bala, G., Bopp, L., Brovkin, V., Canadell, J., et al. (2013). Carbon and
360 Other Biogeochemical Cycles. In T. F. Stocker, D. Qin, G.-K. Plattner, M. Tignor, S. K.
361 Allen, J. Boschung, et al. (Eds.), *Climate Change 2013 - The Physical Science Basis* (pp.
362 465–570). Cambridge, United Kingdom and New York, NY, USA: Cambridge University
363 Press.

364 Davies-Barnard, T., Meyerholt, J., Zaehle, S., Friedlingstein, P., Brovkin, V., Fan, Y., et al.
365 (2020). Nitrogen cycling in CMIP6 land surface models: progress and limitations.
366 *Biogeosciences*, 17, 5129–5148. <https://doi.org/10.5194/bg-17-5129-2020>

367 Dong, Y., Wang, Z., Sun, H., Yang, W., & Xu, H. (2018). The Response Patterns of Arbuscular
368 Mycorrhizal and Ectomycorrhizal Symbionts Under Elevated CO₂: A Meta-Analysis.
369 *Frontiers in Microbiology*, 9. <https://doi.org/10.3389/fmicb.2018.01248>

370 Drake, J. E., Gallet-Budynek, A., Hofmockel, K. S., Bernhardt, E. S., Billings, S. A., Jackson, R.
371 B., et al. (2011). Increases in the flux of carbon belowground stimulate nitrogen uptake and
372 sustain the long-term enhancement of forest productivity under elevated CO₂. *Ecology*
373 *Letters*, 14(4), 349–357. <https://doi.org/10.1111/j.1461-0248.2011.01593.x>

374 Fisher, J. B., Sitch, S., Malhi, Y., Fisher, R. A., Huntingford, C., & Tan, S.-Y. (2010). Carbon
375 cost of plant nitrogen acquisition: A mechanistic, globally applicable model of plant
376 nitrogen uptake, retranslocation, and fixation. *Global Biogeochemical Cycles*, 24(1), n/a-
377 n/a. <https://doi.org/10.1029/2009GB003621>

378 Fisher, R. A., Wieder, W. R., Sanderson, B. M., Koven, C. D., Oleson, K. W., Xu, C., et al.
379 (2019). Parametric Controls on Vegetation Responses to Biogeochemical Forcing in the

- 380 CLM5. *Journal of Advances in Modeling Earth Systems*, 11(9), 2879–2895.
381 <https://doi.org/10.1029/2019MS001609>
- 382 Fleischer, K., Rammig, A., De Kauwe, M. G., Walker, A. P., Domingues, T. F., Fuchslueger, L.,
383 et al. (2019). Amazon forest response to CO₂ fertilization dependent on plant phosphorus
384 acquisition. *Nature Geoscience*, 12(9), 736–741. [https://doi.org/10.1038/s41561-019-0404-](https://doi.org/10.1038/s41561-019-0404-9)
385 9
- 386 Friedlingstein, P., Cox, P., Betts, R., Bopp, L., von Bloh, W., Brovkin, V., et al. (2006). Climate-
387 carbon cycle feedback analysis: Results from the C4MIP model intercomparison. *Journal of*
388 *Climate*. <https://doi.org/10.1175/JCLI3800.1>
- 389 Friedlingstein, P., Meinshausen, M., Arora, V. K., Jones, C. D., Anav, A., Liddicoat, S. K., &
390 Knutti, R. (2014). Uncertainties in CMIP5 Climate Projections due to Carbon Cycle
391 Feedbacks. *Journal of Climate*, 27(2), 511–526. <https://doi.org/10.1175/JCLI-D-12-00579.1>
- 392 Friedlingstein, P., Jones, M. W., O'sullivan, M., Andrew, R. M., Hauck, J., Peters, G.
393 P., et al. (2019). Global Carbon Budget 2019. *Earth System Science Data*, 11(4), 1783–
394 1838. <https://doi.org/10.5194/essd-11-1783-2019>
- 395 Goll, D. S., Winkler, A. J., Raddatz, T., Dong, N., Prentice, I. C., Ciais, P., & Brovkin, V.
396 (2017). Carbon–nitrogen interactions in idealized simulations with JSBACH (version 3.10).
397 *Geoscientific Model Development*, 10(5), 2009–2030. [https://doi.org/10.5194/gmd-10-2009-](https://doi.org/10.5194/gmd-10-2009-2017)
398 2017
- 399 Hedin, L. O., Brookshire, E. N. J., Menge, D. N. L., & Barron, A. R. (2009). The Nitrogen
400 Paradox in Tropical Forest Ecosystems. *Annual Review of Ecology, Evolution, and*
401 *Systematics*, 40(1), 613–635. <https://doi.org/10.1146/annurev.ecolsys.37.091305.110246>
- 402 van der Heijden, M. G. A., Martin, F. M., Selosse, M.-A., & Sanders, I. R. (2015). Mycorrhizal
403 ecology and evolution: the past, the present, and the future. *New Phytologist*, 205(4), 1406–
404 1423. <https://doi.org/10.1111/nph.13288>
- 405 Jo, I., Fei, S., Oswald, C. M., Domke, G. M., & Phillips, R. P. (2019). Shifts in dominant tree
406 mycorrhizal associations in response to anthropogenic impacts. *Science Advances*, 5(4),

- 407 eaav6358. <https://doi.org/10.1126/sciadv.aav6358>
- 408 Keenan, T. F., Prentice, I. C., Canadell, J. G., Williams, C., Wang, H., Raupach, M. R., &
409 Collatz, G. J. (2016). Recent pause in the growth rate of atmospheric CO₂ due to enhanced
410 terrestrial carbon uptake. *Nature Communications*. <https://doi.org/10.1038/ncomms13428>
- 411 Kennedy, D., Swenson, S., Oleson, K. W., Lawrence, D. M., Fisher, R., Lola da Costa, A. C., &
412 Gentine, P. (2019). Implementing Plant Hydraulics in the Community Land Model, Version
413 5. *Journal of Advances in Modeling Earth Systems*, *11*(2), 485–513.
414 <https://doi.org/10.1029/2018MS001500>
- 415 Kim, H. (2017). Global Soil Wetness Project Phase 3 Atmospheric Boundary Conditions
416 (Experiment 1). Data Integration and Analysis System (DIAS).
417 <https://doi.org/https://doi.org/10.20783/DIAS.501>
- 418 Kivlin, S. N., Emery, S. M., & Rudgers, J. A. (2013). Fungal symbionts alter plant responses to
419 global change. *American Journal of Botany*, *100*(7), 1445–1457.
420 <https://doi.org/10.3732/ajb.1200558>
- 421 Kolus, H. R., Huntzinger, D. N., Schwalm, C. R., Fisher, J. B., McKay, N., Fang, Y., et al.
422 (2019). Land carbon models underestimate the severity and duration of drought's impact on
423 plant productivity. *Scientific Reports*, *9*(1), 2758. [https://doi.org/10.1038/s41598-019-](https://doi.org/10.1038/s41598-019-39373-1)
424 [39373-1](https://doi.org/10.1038/s41598-019-39373-1)
- 425 Kriegler, E., Bauer, N., Popp, A., Humpenöder, F., Leimbach, M., Strefler, J., et al. (2017).
426 Fossil-fueled development (SSP5): An energy and resource intensive scenario for the 21st
427 century. *Global Environmental Change*, *42*, 297–315.
428 <https://doi.org/10.1016/j.gloenvcha.2016.05.015>
- 429 Lawrence, D. M., Hurtt, G. C., Arneth, A., Brovkin, V., Calvin, K. V., Jones, A. D., et al. (2016).
430 The Land Use Model Intercomparison Project (LUMIP) contribution to CMIP6: rationale
431 and experimental design. *Geoscientific Model Development*, *9*(9), 2973–2998.
432 <https://doi.org/10.5194/gmd-9-2973-2016>
- 433 Lawrence, D. M., Fisher, R. A., Koven, C. D., Oleson, K. W., Swenson, S. C., Bonan, G., et al.

- 434 (2019). The Community Land Model Version 5: Description of New Features,
435 Benchmarking, and Impact of Forcing Uncertainty. *Journal of Advances in Modeling Earth*
436 *Systems*, 11(12), 4245–4287. <https://doi.org/10.1029/2018MS001583>
- 437 McGroddy, M. E., Daufresne, T., & Hedin, L. O. (2004). Scaling of C:N:P stoichiometry in
438 forests worldwide: implications of terrestrial redfield-type ratios. *Ecology*, 85(9), 2390–
439 2401. <https://doi.org/10.1890/03-0351>
- 440 Menzel, A., Hempel, S., Manceur, A. M., Götzenberger, L., Moora, M., Rillig, M. C., et al.
441 (2016). Distribution patterns of arbuscular mycorrhizal and non-mycorrhizal plant species
442 in Germany. *Perspectives in Plant Ecology, Evolution and Systematics*, 21, 78–88.
443 <https://doi.org/10.1016/j.ppees.2016.06.002>
- 444 NCAR. (2019). CLM5 Documentation Release, 337.
- 445 NCAR. (2020). CHEYENNE. <https://doi.org/10.5065/D6RX99HX>
- 446 Norby, R. J., De Kauwe, M. G., Walker, A. P., Werner, C., Zaehle, S., & Zak, D. R. (2017).
447 Comment on “Mycorrhizal association as a primary control of the CO₂ fertilization effect.”
448 *Science*, 355(6323), 358.2-358. <https://doi.org/10.1126/science.aai7976>
- 449 O’Neill, B. C., Tebaldi, C., Van Vuuren, D. P., Eyring, V., Friedlingstein, P., Hurtt, G., et al.
450 (2016). The Scenario Model Intercomparison Project (ScenarioMIP) for CMIP6.
451 *Geoscientific Model Development*, 9(9), 3461–3482. [https://doi.org/10.5194/gmd-9-3461-](https://doi.org/10.5194/gmd-9-3461-2016)
452 2016
- 453 Orwin, K. H., Kirschbaum, M. U. F., St John, M. G., & Dickie, I. A. (2011). Organic nutrient
454 uptake by mycorrhizal fungi enhances ecosystem carbon storage: a model-based
455 assessment. *Ecology Letters*, 14(5), 493–502. [https://doi.org/10.1111/j.1461-](https://doi.org/10.1111/j.1461-0248.2011.01611.x)
456 0248.2011.01611.x
- 457 Reich, P. B., & Oleksyn, J. (2004). Global patterns of plant leaf N and P in relation to
458 temperature and latitude. *Proceedings of the National Academy of Sciences*, 101(30),
459 11001–11006. <https://doi.org/10.1073/pnas.0403588101>

- 460 Reich, Peter B., Sendall, K. M., Rice, K., Rich, R. L., Stefanski, A., Hobbie, S. E., &
461 Montgomery, R. A. (2015). Geographic range predicts photosynthetic and growth response
462 to warming in co-occurring tree species. *Nature Climate Change*, 5(2), 148–152.
463 <https://doi.org/10.1038/nclimate2497>
- 464 Riahi, K., van Vuuren, D. P., Kriegler, E., Edmonds, J., O'Neill, B. C., Fujimori, S., et al.
465 (2017). The Shared Socioeconomic Pathways and their energy, land use, and greenhouse
466 gas emissions implications: An overview. *Global Environmental Change*, 42, 153–168.
467 <https://doi.org/10.1016/j.gloenvcha.2016.05.009>
- 468 Schimel, D., Stephens, B. B., & Fisher, J. B. (2015). Effect of increasing CO₂ on the terrestrial
469 carbon cycle. *Proceedings of the National Academy of Sciences*, 112(2), 436–441.
470 <https://doi.org/10.1073/pnas.1407302112>
- 471 Shi, M., Fisher, J. B., Brzostek, E. R., & Phillips, R. P. (2016). Carbon cost of plant nitrogen
472 acquisition: global carbon cycle impact from an improved plant nitrogen cycle in the
473 Community Land Model. *Global Change Biology*, 22(3), 1299–1314.
474 <https://doi.org/10.1111/gcb.13131>
- 475 Smith, M. R., & Myers, S. S. (2018). Impact of anthropogenic CO₂ emissions on global human
476 nutrition. *Nature Climate Change*, 8(9), 834–839. [https://doi.org/10.1038/s41558-018-0253-](https://doi.org/10.1038/s41558-018-0253-3)
477 3
- 478 Soudzilovskaia, N. A., van Bodegom, P. M., Terrer, C., Zelfde, M. van't, McCallum, I., Luke
479 McCormack, M., et al. (2019). Global mycorrhizal plant distribution linked to terrestrial
480 carbon stocks. *Nature Communications*, 10(1), 5077. [https://doi.org/10.1038/s41467-019-](https://doi.org/10.1038/s41467-019-13019-2)
481 13019-2
- 482 Steidinger, B. S., Crowther, T. W., Liang, J., Van Nuland, M. E., Werner, G. D. A., Reich, P. B.,
483 et al. (2019). Climatic controls of decomposition drive the global biogeography of forest-
484 tree symbioses. *Nature*, 569(7756), 404–408. <https://doi.org/10.1038/s41586-019-1128-0>
- 485 Sulman, B. N., Brzostek, E. R., Medici, C., Shevliakova, E., Menge, D. N. L., & Phillips, R. P.
486 (2017). Feedbacks between plant N demand and rhizosphere priming depend on type of

- 487 mycorrhizal association. *Ecology Letters*, 20(8), 1043–1053.
488 <https://doi.org/10.1111/ele.12802>
- 489 Sulman, B. N., Shevliakova, E., Brzostek, E. R., Kivlin, S. N., Malyshev, S., Menge, D. N. L., &
490 Zhang, X. (2019). Diverse Mycorrhizal Associations Enhance Terrestrial C Storage in a
491 Global Model. *Global Biogeochemical Cycles*, 33(4), 501–523.
492 <https://doi.org/10.1029/2018GB005973>
- 493 Swaty, R., Michael, H. M., Deckert, R., & Gehring, C. A. (2016). Mapping the potential
494 mycorrhizal associations of the conterminous United States of America. *Fungal Ecology*,
495 24, 139–147. <https://doi.org/10.1016/j.funeco.2016.05.005>
- 496 Terrer, C., Vicca, S., Hungate, B. A., Phillips, R. P., & Prentice, I. C. (2016). Mycorrhizal
497 association as a primary control of the CO₂ fertilization effect. *Science*, 353(6294), 72–74.
498 <https://doi.org/10.1126/science.aaf4610>
- 499 Terrer, C., Vicca, S., Stocker, B. D., Hungate, B. A., Phillips, R. P., Reich, P. B., et al. (2018).
500 Ecosystem responses to elevated CO₂ governed by plant-soil interactions and the cost of
501 nitrogen acquisition. *New Phytologist*, 217(2), 507–522. <https://doi.org/10.1111/nph.14872>
- 502 Terrer, C., Jackson, R. B., Prentice, I. C., Keenan, T. F., Kaiser, C., Vicca, S., et al. (2019).
503 Nitrogen and phosphorus constrain the CO₂ fertilization of global plant biomass. *Nature*
504 *Climate Change*, 9(9), 684–689. <https://doi.org/10.1038/s41558-019-0545-2>
- 505 Trenberth, K. E., Dai, A., van der Schrier, G., Jones, P. D., Barichivich, J., Briffa, K. R., &
506 Sheffield, J. (2014). Global warming and changes in drought. *Nature Climate Change*, 4(1),
507 17–22. <https://doi.org/10.1038/nclimate2067>
- 508 Wang, Y. P., Law, R. M., & Pak, B. (2010). A global model of carbon, nitrogen and phosphorus
509 cycles for the terrestrial biosphere. *Biogeosciences*, 7(7), 2261–2282.
510 <https://doi.org/10.5194/bg-7-2261-2010>
- 511 Wieder, W. R., Cleveland, C. C., Smith, W. K., & Todd-Brown, K. (2015). Future productivity
512 and carbon storage limited by terrestrial nutrient availability. *Nature Geoscience*, 8(6), 441–
513 444. <https://doi.org/10.1038/ngeo2413>

514 Wieder, W. R., Lawrence, D. M., Fisher, R. A., Bonan, G. B., Cheng, S. J., Goodale, C. L., et al.
515 (2019). Beyond static benchmarking: Using experimental manipulations to evaluate land
516 model assumptions. *Global Biogeochemical Cycles*. <https://doi.org/10.1029/2018GB006141>

517 Zaehle, S., Friedlingstein, P., & Friend, A. D. (2010). Terrestrial nitrogen feedbacks may
518 accelerate future climate change. *Geophysical Research Letters*, 37(1), n/a-n/a.
519 <https://doi.org/10.1029/2009GL041345>

520 Zaehle, S., Jones, C. D., Houlton, B., Lamarque, J.-F., & Robertson, E. (2015). Nitrogen
521 Availability Reduces CMIP5 Projections of Twenty-First-Century Land Carbon Uptake.
522 *Journal of Climate*, 28(6), 2494–2511. <https://doi.org/10.1175/JCLI-D-13-00776.1>

523 Zhang, Y., Song, C., Band, L. E., & Sun, G. (2019). No Proportional Increase of Terrestrial
524 Gross Carbon Sequestration From the Greening Earth. *Journal of Geophysical Research:*
525 *Biogeosciences*, 2018JG004917. <https://doi.org/10.1029/2018JG004917>

526 Zhu, Z., Piao, S., Myneni, R. B., Huang, M., Zeng, Z., Canadell, J. G., et al. (2016). Greening of
527 the Earth and its drivers. *Nature Climate Change*. <https://doi.org/10.1038/NCLIMATE3004>

528

529

530

531

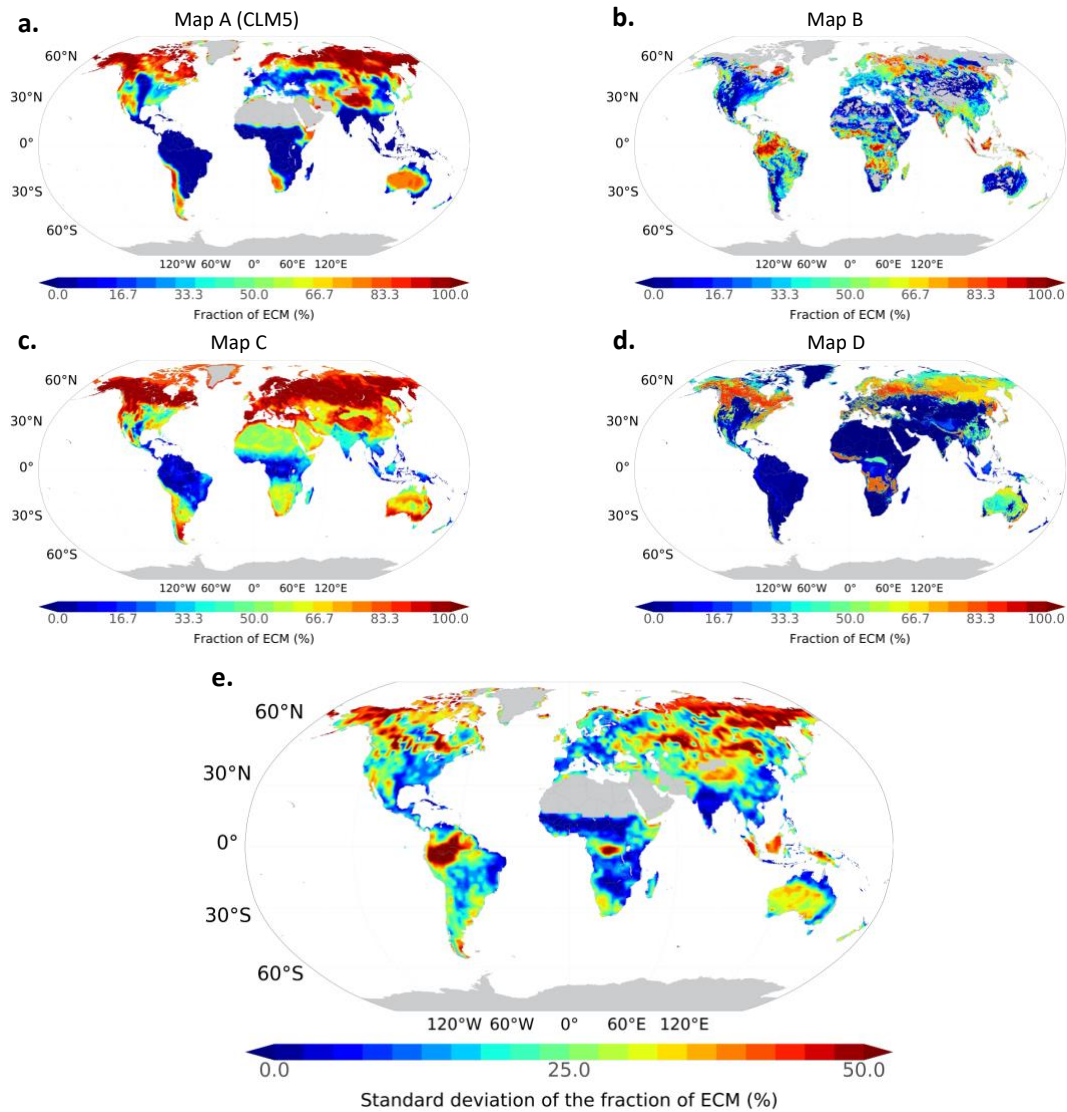
532

533

534

535

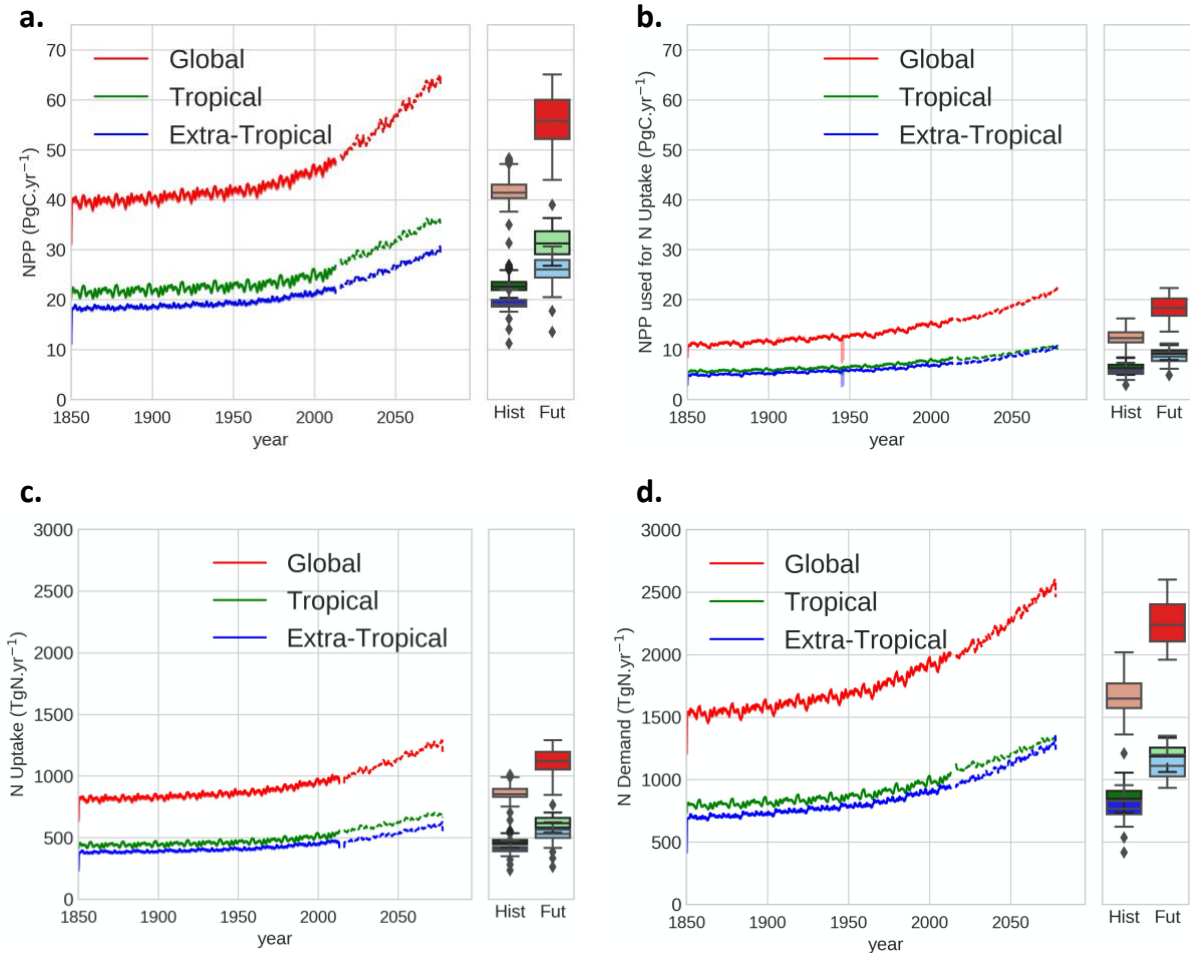
536



537

538 **Figure 1.** Global spatial distributions of ECM fraction (%). The remaining fraction is assumed to
 539 be AM. **a.** Map A (Shi et al., 2016) (look-up table x PFTs in 1.9°x2.5°); **b.** Map B (Sulman et al.,
 540 2019) (0.17°x0.17°); **c.** Map C (Steidinger et al., 2019) (1.0°x1.0° unmasked); and **d.** Map D
 541 (Soudzilovskaia et al., 2019) (0.17°x0.17°); and **e.** standard deviation of all the four maps of ECM
 542 fraction.

543

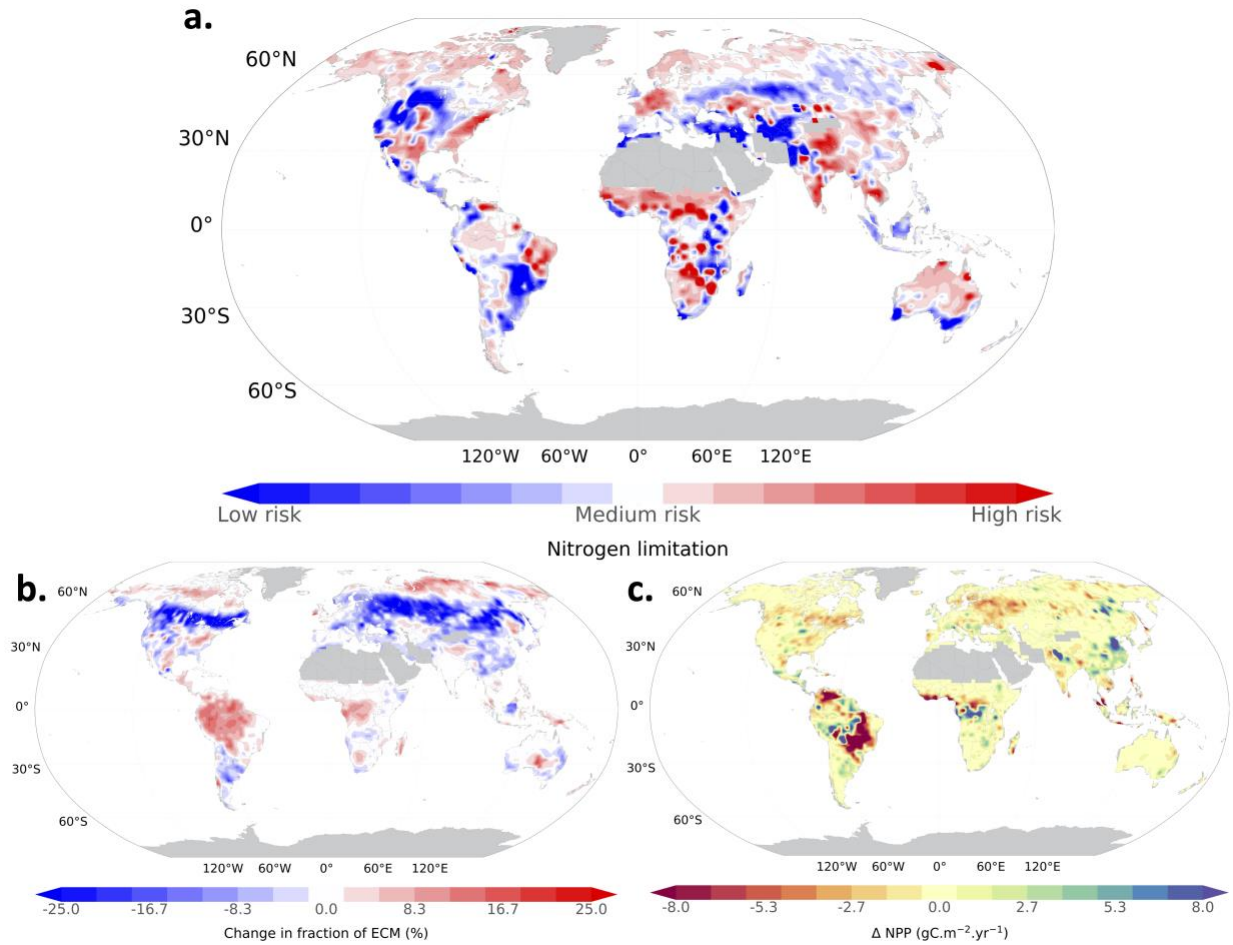


544

545 **Figure 2.** Trend in Net Primary Productivity and usage for nitrogen acquisition **a.** Global total
 546 NPP (PgC.yr^{-1}); **b.** global total carbon cost of nitrogen uptake (NPP_NUPTAKE , PgC.yr^{-1}); **c.**
 547 trend in nitrogen uptake and demand **a.** Global average nitrogen uptake (NUPTAKE , TgN.yr^{-1});
 548 and **d.** global average plant nitrogen demand (PLANT_NDEMAND , TgN.yr^{-1}) for the transient
 549 historical run from 1850 to 2010 (continuous) and for the future projection SSP5 with RCP8.5 run
 550 from 2015 to 2070 (dashed) with CLM5. Tropical stands for the area of the globe between 23.5°S
 551 and 23.5°N . Extra-Tropical is the remaining area of the globe ($90^\circ\text{S}-23.5^\circ\text{S}$ and $23.5^\circ\text{N}-90^\circ\text{N}$).

552

553



554

555

556

557

558

559

560

561

562

Figure 3. a. Risk of nitrogen limitation. Areas in red indicate higher risk of nitrogen limitation on NPP, and areas in blue indicate lower risk of nitrogen limitation on NPP; and projected differences in NPP and mycorrhizae driven by climate change; **b.** The impact of climate change on ECM fraction (%) derived from Steidinger et al. (2019) for 2070 following the RCP8.5 with CMIP5 simulations; **c.** Difference in NPP ($\text{gC}\cdot\text{m}^{-2}\cdot\text{yr}^{-1}$) for future simulations (2016-2075) between projected future map generated for the year of 2070 and the present-day map C (Steidinger et al., 2019). The projected runs with CLM5 followed the SSP5 scenario in combination with RCP8.5 climate forcing from CESM, member of CMIP6 simulations.